

Contrasting stratospheric–tropospheric multi-fractal behaviors in NAM variability

Da Nian & Zuntao Fu

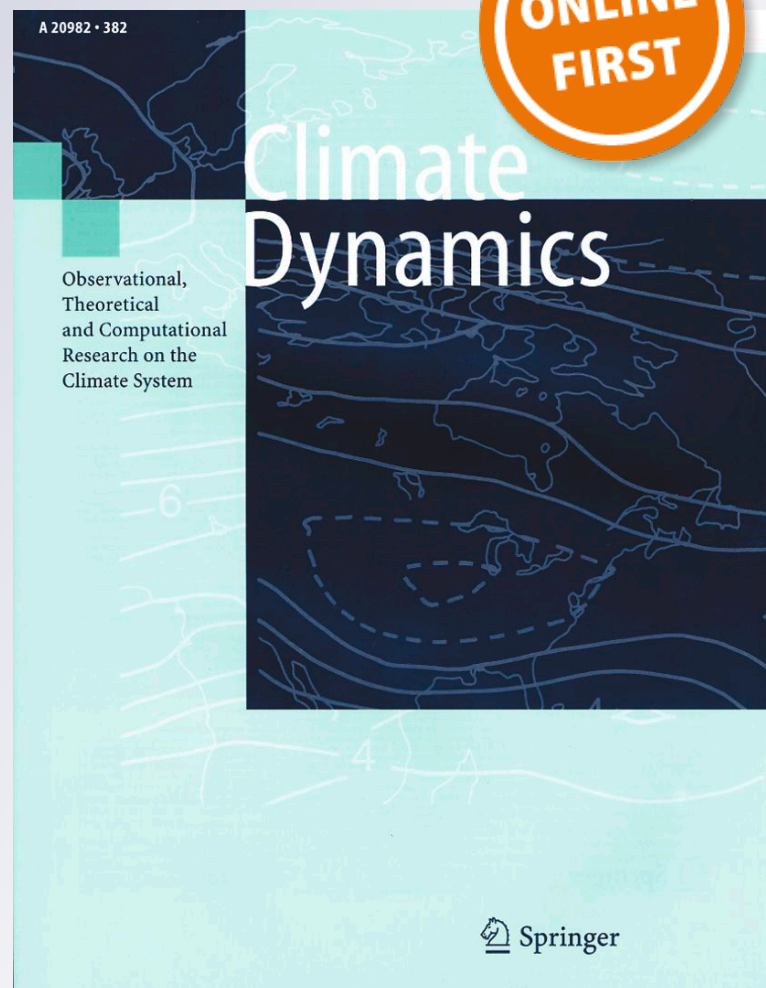
Climate Dynamics

Observational, Theoretical and
Computational Research on the Climate
System

ISSN 0930-7575

Clim Dyn

DOI 10.1007/s00382-019-04981-0



Your article is protected by copyright and all rights are held exclusively by Springer-Verlag GmbH Germany, part of Springer Nature. This e-offprint is for personal use only and shall not be self-archived in electronic repositories. If you wish to self-archive your article, please use the accepted manuscript version for posting on your own website. You may further deposit the accepted manuscript version in any repository, provided it is only made publicly available 12 months after official publication or later and provided acknowledgement is given to the original source of publication and a link is inserted to the published article on Springer's website. The link must be accompanied by the following text: "The final publication is available at link.springer.com".



Contrasting stratospheric–tropospheric multi-fractal behaviors in NAM variability

Da Nian¹ · Zuntao Fu¹ Received: 3 January 2019 / Accepted: 9 September 2019
© Springer-Verlag GmbH Germany, part of Springer Nature 2019

Abstract

As a harbinger of anomalous weather regimes in the troposphere, the Northern Annular Mode (NAM) propagates from the stratosphere to the troposphere. This fact makes understanding and predicting NAM variability of great importance. In this study, the multi-fractal behaviors of NAM variability are investigated using extended self-similarity based, multi-fractal detrended fluctuation analysis (ESS-MF-DFA) and the NAM indices from 1000 to 10 hPa. The results show that there are contrasting multi-fractal behaviors between the stratosphere and the troposphere that have a transition band near 200 hPa. The stratospheric NAM variability is more complicated and has multiple multi-fractal regimes over different scales with marked contrasting warm–cold season features. To understand these contrasting stratospheric–tropospheric multi-fractal behaviors, three surrogate methods are adopted to show how temporal ordinal patterns over an annual scale contribute to these behaviors, whereas the distribution of NAM variability only plays a minor role. Further studies show that contrasting warm–cold variability may lead to these contrasting behaviors. Among them, warm–cold seasonal variations, power spectral density (PSD), and autocorrelation provide a similar conclusion. Results indicate that although predictions of the NAM index over the stratosphere are required and necessary, the complicated multi-fractal behaviors make linear prediction strategy difficult to obtain high realizable predictability of NAM variations over the stratosphere.

Keywords Northern Annular Mode (NAM) · Multiple multi-fractal behavior · Stratospheric–tropospheric variability · Warm–cold season variations

1 Introduction

The Northern Annular Mode (NAM), which reflects one of the main atmospheric variabilities in the extratropical Northern Hemisphere, represents a dipole phenomenon of atmospheric mass between high and low latitudes in the earth's hemisphere (Limpasuvan and Hartmann 1999). It is also called the Arctic Oscillation (AO) (Thompson and Wallace 1998). The concept of this 'Annular Mode,' which characterizes the cardinal pattern of extra-altitude atmospheric circulation and facilitates an understanding of the Arctic climate mode, is also called the North's 'El Niño' (Kerr 2001). This variability possesses a clear spatial pattern, has a major temporal variation that is

estimated using the NAM index, and is associated with some crucial climatic and synoptic activities (Kerr 1999; Limpasuvan and Hartmann 2000). An increasing number of studies have shown that the relationship of the oscillations between the stratosphere and troposphere plays a key role in predicting anomalous weather (Baldwin and Dunkerton 2001; Baldwin et al. 2003; Baldwin and Thompson 2009; Stockdale et al. 2015; Wang et al. 2017). The anomalies of NAM/AO from the stratosphere can propagate to the troposphere (Cai and Ren 2007), which can facilitate a realization of a 10-day to 30-day sub-seasonal prediction (Baldwin and Dunkerton 2001; Baldwin et al. 2003; Thompson et al. 2002). There is also evidence that stratosphere-troposphere interactions can induce persistent intra-seasonal dynamics, displaying enhanced persistence on intra-seasonal timescales (Ambaum and Hoskins 2002; Baldwin et al. 2003). By adjusting the strength and the frequency of related atmospheric activities, NAM/AO manifests strong impacts on climate variables in winter, such as temperature, precipitation, sea ice, and snow cover; this

✉ Zuntao Fu
fuzt@pku.edu.cn

¹ Lab for Climate and Ocean-Atmosphere Studies, Department of Atmospheric and Oceanic Sciences, School of Physics, Peking University, Beijing 100871, China

is evidenced not only through mean variations, but also in daily changes (Thompson and Wallace 1998, 2001; Wang and Ikeda 2000; Bamzai 2003; Gong et al. 2007). NAM/AO is also related to monsoons, the Siberian High, and extreme events in the Northern Hemisphere (Gong et al. 2001). For example, during the winter of 2009–2010 with extreme cold and snow in most major cities of industrialized countries of the Northern Hemisphere, the explained variance from NAM/AO contributed more than that from ENSO to the observed temperature mode over mid-latitudes (Cohen et al. 2010). As such, there is a potential application for predicting variations in the NAM index; however, this requires a comprehensive understanding of the behaviors of the NAM/AO.

In general, it is not simple to predict the NAM index at a seasonal scale. The seasonal hindcasting results from the Climate Forecast System version 2 (CFSv2) have shown that the correlation skills of predicting the NAM/AO anomaly can be greater than 0.5 in a one-month lead forecast over a 28-year period (Riddle et al. 2013). Subsequently, a simulation performed by Sun and Ahn (2015) revealed the dynamic seasonal predictability of NAM/AO using a coupled general circulation model. In addition, Stockdale et al. (2015) examined the predictability of several operational forecast models for NAM/AO and found that a high-skilled predictable correlation reached 0.61 from 1981 to 2010. Domeisen et al. (2018) calculated the predictability time scales of daily NAO and AO indices and found that the predictability exceeded the short-term predictability; this can be currently obtained using the ensemble prediction model. These results indicated that there is room for improvement in predicting the NAM index over different time scales.

What can be done to improve prediction ability? A thorough understanding of the nonlinear characteristics of NAM/AO may provide some insight. In recent studies, one of the most crucial reasons for the difficulty of NAM/AO variation predictions is the nonlinearities and complexities of the system. These apparent nonlinearities in the NAM index restrict the performance of models that primarily use correlations to identify predictability (Stockdale et al. 2015). However, Ye and Hsieh (2008) found that increasing nonlinearity in the ENSO and Lorenz systems could help to enhance the predictability. Even though nonlinear items in the dynamic controlling equations can reduce predictability, they can lead to longer-period oscillations in the ENSO and Lorenz systems that can induce great potential predictability. It is exciting to find that the NAM variability has a chaotic origin, and the spectrum of the NAM index in 1000 hPa is more consistent with low-order chaos (Osprey and Ambaum 2011). In addition, Hirata et al. (2011) testified this nonlinearity and chaos in the AO index using statistical toy models. Therefore, the nonlinearities in NAM variability may have an impact on prediction.

Given that the primary purpose is to understand and improve predictability of the NAM index, the nonlinearity over different time scales could be an important area that requires focused attention. Previous studies have suggested that there are distinct behaviors over various timescale ranges in the North Atlantic Oscillation (NAO) index (Keenly et al. 2009). The characteristic of inter-annual variability in the NAO index can reflect influences from external factors, such as changes in radiation forcing or the tropic Indo-Pacific sea surface temperature (Gillett et al. 2003; Hoerling et al. 2001). Moreover, Badin and Domeisen (2014a) found that the behavior of stratospheric variability in the Northern Hemisphere is chaotic. The stratospheric variability exhibits different chaotic behaviors in the Northern and Southern Hemisphere (Badin and Domeisen 2014b). There is some independence among the Annular Modes between the stratosphere and the troposphere, sometimes with opposite changes (Baldwin and Dunkerton 1999) that may induce different scaling behaviors. However, the coupling between polar stratospheric events and mid-latitude tropospheric events is a key feature of observed variability, and these events are associated with the time scale of the NAM index. The increased variability of the Annular Mode in the stratosphere has a close relationship with the increased persistence of the Annular Mode in the troposphere (Gerber et al. 2010). Simpson et al. (2011) quantified the impact of stratospheric variability on the time scale of the tropospheric Annular Mode. In both hemispheres, the effect of stratospheric variability on extending the time scale of the tropospheric Annular Mode was clear. However, only a few studies have directly investigated the nonlinearity or chaotic behavior over different timescales in detail. Badin and Domeisen (2016) studied different scaling laws and multi-fractal features of different stratospheric variabilities and found that there was a transition in the scaling exponent at time scales shorter than approximately 1 year. To learn more about the physical processes or potential predictability of the NAM index, a multi-fractal measure was also adopted (Kantelhardt et al. 2002) that quantifies a scaling behavior using different behaviors at different time scales. If the scaling behavior at different time scales is different, then it is multi-fractal, and the opposite is mono-fractal (two-point linear long-term persistence).

The nonlinearity difference in the stratosphere and troposphere cannot be ignored. Fu et al. (2016) indicated that nonlinearities increase as the pressure level decreases. More specifically, the NAM indices over different heights demonstrate various nonlinear characteristics. These results imply that the multi-fractal behavior of the NAM index at different heights should receive more attention because it is one of the important indicators of nonlinearity. This study investigates the NAM indices over 17 pressure levels, from 1000 to 10 hPa, during the 1948–2017 time period. Given the

availability of these long time series, the following questions are addressed:

1. What is the multi-fractal behavior of the NAM indices at various pressure levels? Is the behavior mono-fractal or multi-fractal?
2. If it is multi-fractal, what is the origin of the multi-fractal behavior?
3. Are there different multi-fractal behaviors in the stratospheric and tropospheric NAM variability?
4. If the answer is yes, how can researchers understand this contrasting multi-fractal behavior and its implications?

2 Data and methods

2.1 Data source and processing

The data we used in this study were daily geo-potential height fields downloaded from the National Centers for Environmental Prediction–National Center for the Atmospheric Research (NCEP/NCAR) reanalysis project (Kalnay et al. 1996). This variable was on a $2.5^\circ \times 2.5^\circ$ grid for the period from 1948 to 2017 and was available from 1000 to 10 h Pa over 17 levels. The dataset from the Japanese 55-year Reanalysis (JRA-55) project conducted by the Japan Meteorological Agency (JMA) was also used for testing the robustness of the results, which was a $2.5^\circ \times 2.5^\circ$ grid for the period from 1958 to 2017 with 37 levels (Kobayashi et al. 2015). NAM indices at each level were calculated following the method of Baldwin and Dunkerton (Baldwin and Dunkerton 2001) by selecting the December to February geopotential height data and removing the annual cycle (the value of each calendar day was the average of the same day for all years). For each pressure level, the Empirical Orthogonal Function (EOF) patterns were calculated using wintertime (December–February) monthly mean data north of 20°N . Finally, the daily geopotential anomalies were projected onto the leading EOF patterns (Fu et al. 2016). This process considered the impact from weightings of the latitude. Four typical normalized daily NAM indices (subtract its mean value and divide by its standard deviation) at 1000 hPa, 200 hPa, 100 hPa, and 10 hPa are illustrated in Fig. 1.

2.2 Methods

A multi-fractal analysis is an effective way to describe the nonlinearity hidden in a time series. The most common way to estimate this feature is the multi-fractal detrended fluctuation analysis (MF-DFA) method. However, this method does not perform well for the NAM index, where the basic power law assumption is not satisfied for the detrended fluctuation analysis (DFA) and the MF-DFA (Fu et al. 2016). In this

case, a novel quantifying method, called the extended self-similarity-based multi-fractal detrended fluctuation analysis (ESS-MF-DFA), can solve this problem and be used to analyze the multi-fractal behavior in the NAM index (Nian and Fu 2019).

In this subsection, the algorithm of the ESS-MF-DFA method is briefly explained (Nian and Fu 2019). By considering a time series $[x(t), t = 1, 2, 3, \dots, N]$ with a zero mean and calculating the profile of $[x(t)]$, the profile function, $y(t)$, can be cut into N_s isometric segments. Here $y(t) = \sum_{i=1}^t [x(i) - \langle x \rangle]$ and $\langle x \rangle = \frac{1}{N} \sum_{i=1}^N x(i)$ is the mean value of the time series. By applying the same process repeatedly starting from the opposite end, we can obtain $2N_s$ segments in total. Thereby, the variance of each segment is:

$$F^2(v, s) = \frac{1}{s} \sum_{i=1}^s \{y[(v-1)s+i] - t_v(i)\}^2, \quad (1)$$

where $t_v(i)$ is the trend of segment v , fitted using three order polynomials. Then, the q th order fluctuation function averaged over all segments is:

$$F_q(s) \equiv \left\{ \frac{1}{2N_s} \sum_{v=1}^{2N_s} \left[F^2(v, s)^{\frac{q}{2}} \right]^{\frac{1}{q}} \right\}, \quad (2)$$

where q can take any real value. However, when $q = 0$, the fluctuation function should be calculated using another average procedure:

$$F_0(s) = \exp \left\{ \frac{1}{4N_s} \sum_{v=1}^{2N_s} \ln[F^2(v, s)] \right\} \sim s^{H(0)}. \quad (3)$$

Given the fluctuation function satisfies the power law assumption, from Eqs. (2) and (3), we have:

$$\log_{10} F_q(s) \sim H(q) \log_{10} s, \quad (4)$$

where s is the scale value, and $H(q)$ is the generalized Hurst exponent.

The fluctuation functions of various q satisfy the following:

$$\log_{10}(F_q(s)) \sim A_{q,q'} \log_{10}(F_{q'}(s)), \quad A_{q,q'} = \frac{H(q)}{H(q')} \quad (5)$$

where q and q' can be different, and $H(q') \neq 0$. $A_{q,q'}$ can be estimated directly by the slope of $\log_{10}(F_q(s))$ versus $\log_{10}(F_{q'}(s))$ in the plot. In this article, $q' = 2$ was chosen. That is, $A_{q,q'} = A_{q,2}$, and abbreviated as A_q . Also, A_q describes the scaling behavior of larger fluctuations relative to $q = 2$ when q is positive, while it describes the scaling behavior of small fluctuations relative to $q = 2$ when q is negative. Therefore, if $A(q)$ is independent of q , the scaling

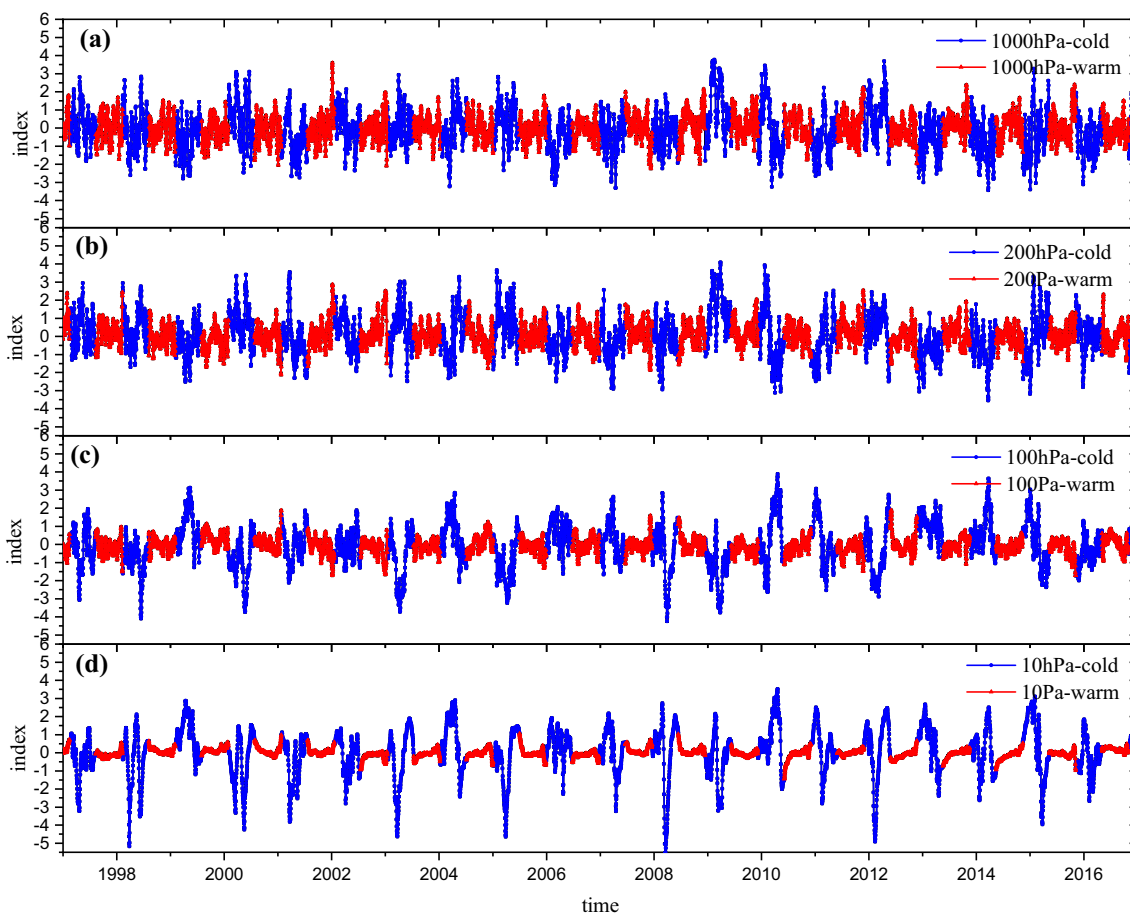


Fig. 1 Typical NAM index series at four pressure levels: **a** 1000 hPa, **b** 200 hPa, **c** 100 hPa and **d** 10 hPa. The blue lines represent the cold half year (November, December, January, February, March, April),

and the red lines represent the warm half year (May, June, July, August, September, October). All of the series are normalized

behavior of the entire fluctuation is the same; that is, the time series has a mono-fractal property.

Then the multi-fractal strength through ΔA_q with a finite range of q can be evaluated:

$$\Delta A_q = \max A_q - \min A_q. \tag{6}$$

In this study, let $q = -3, -2, -1, 0, 1, 2, 3$.

For MF-DFA, the results depend on the difference of the generalized Hurst exponent varying with q , which depends on the power law assumption in the DFA procedure. However, for some situations (e.g. wind speed of the boundary layer, the NAM index), the power law assumption between the fluctuation function and the scale in the DFA method fails, causing the result using MF-DFA to have bias in the estimate of the multifractal strength. As for ESS-MF-DFA, even the power law assumption is not satisfied in Eq. (4). This may still exist the relation of Eq. (5) among the fluctuation functions of various q . In other words, even if the fluctuation function of DFA does not change in a power

law form with the scale, the multifractal features can still be quantified using the relation of Eq. (5).

3 Results

3.1 Multi-fractal behaviors in NAM variability

3.1.1 NAM variability over different pressure levels

A significant variability difference between the large fluctuation and the small fluctuation of the NAM index appeared in the stratosphere, while this difference was weak in the troposphere (as shown in Fig. 1). Figure 1 shows that the lower the pressure level, the stronger the difference in the fluctuations of the NAM index time series, which is similar to the results found by Fu et al. (2016). The NAM variability in the middle level of the stratosphere represents the

strength of the polar vortex (Baldwin and Dunkerton 1999; Baldwin et al. 2003). It is clear from the figure that the large fluctuation in the NAM index changed more slowly in the stratosphere around 10 hPa than it did in the lower troposphere at approximately 1000 hPa, which corresponds to the polar vortex result reported by Cai and Ren (2007). Different changing features between large and small fluctuations represent clear multi-fractal properties in the NAM indices. To explore this multi-fractal behavior, the ESS-MF-DFA method was used.

3.1.2 Complicated and multiple scaling properties in NAM variability

The results of the ESS-MF-DFA method illustrated in Fig. 2 show that NAM variability is multi-fractal over all pressure levels since the ESS-MF-DFA results for each q are scattered and not collapsed. There exist many complicated multi-fractal behaviors in the NAM indices. This is illustrated more precisely in Fig. 3, with the local slope in the log–log plot of $F_q(s)$ versus $F_2(s)$ calculated with a moving window size of eight points. According to Nian and Fu (2019), the ideal local slopes for a typical multi-fractal time series with only one scaling range should be constants for each q . More precisely, there should only be a plateau with

its own specific value in the local slope for each q over the entire range. The multi-fractal strength can be quantified by the dispersion of plateaus for all q , and the larger the multi-fractal strength, the greater the distance is between the maximum and minimum local slope. If the underlying series is mono-fractal, then all local slopes collapse into a single plateau with the same value. However, for NAM variability, there are approximately three scaling regimes with break points near $s = 10^2$ and $s = 10^3$ for local slope A over the entire range. The middle part shows a unique strong ΔA , increasing from 100 to 10 hPa, and reaching a maximum of 2.28 at 10 hPa. It should be noted that the plateau is not clear over certain levels, especially for the higher levels over the stratosphere. This is due to a narrower scaling range and moving window size, which makes the plateau invisible in this middle range. The ΔA in the first portion is estimated to be 0.21 and the last part is 0.27. The criteria of mono- or multi-fractal series are $\Delta_{0.95} \approx 0.05$ (Nian and Fu 2019). In more precise terms, the NAM variability over all pressure levels is multi-fractal, with similar multi-fractal strengths at a small scale range from approximately $s = 10$ to approximately $s = 10^2$ and a large scale range from approximately $s = 10^2$ to approximately $s = 10^3$. However, the maximum strength is near the scale of $s = 345$ in the middle range. Badin and Domeisen (2016) also studied the multi-fractal

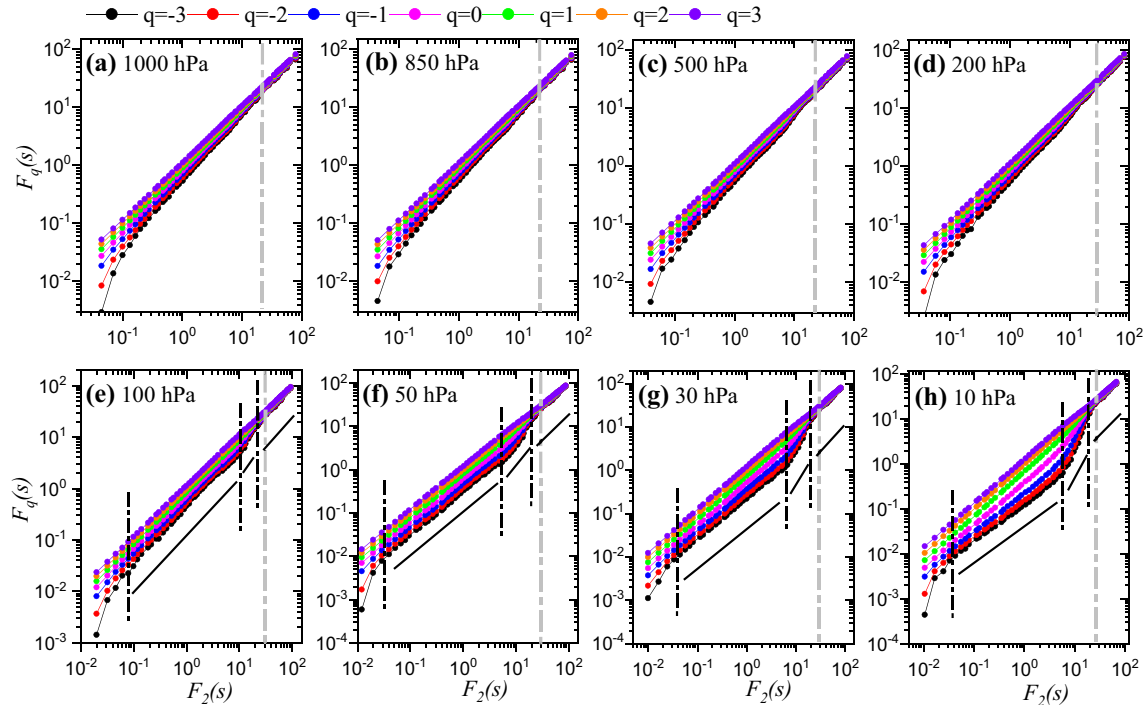


Fig. 2 The ESS-MF-DFA results with q ($q = -3, -2, -1, 0, 1, 2, 3$) for the NAM index series at various pressure levels: **a** 1000 hPa, **b** 850 hPa, **c** 500 hPa, **d** 200 hPa, **e** 100 hPa, **f** 50 hPa, **g** 30 hPa, **h** 10 hPa. The grey dashed line represents the same position in Fig. 11

with the x axis of the scale s . The black dashed lines indicate different regimes with various multi-fractal behaviors when the pressure level is above 100 hPa

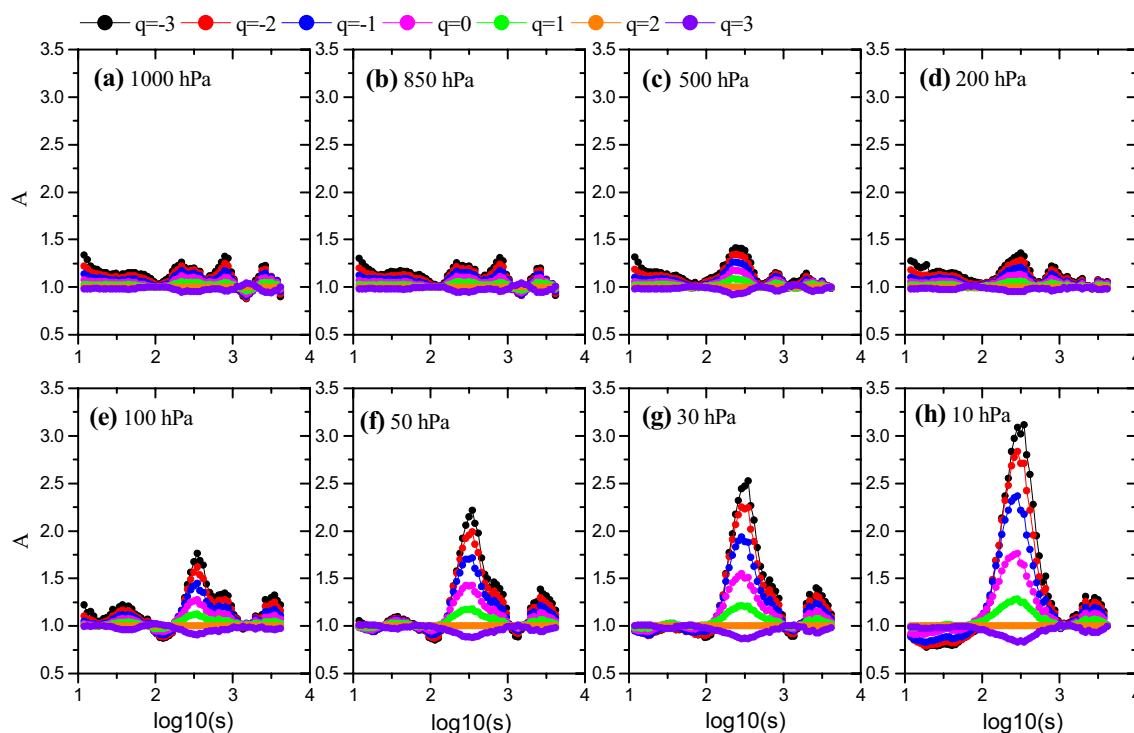


Fig. 3 The local slope (A) in Fig. 2. The largest slope difference within a given interval q ($\Delta A = \max A_q - \min A_q$) means the multi-fractal strength in the series

features of stratospheric variability at 10 hPa and found two scaling regimes with a transition of scaling exponents shorter than approximately one year, which is similar to the result in this study (345 days). The first and second regimes of the result in this study are roughly equivalent to the first regime of Badin and Domeisen's result. This difference is because the method used in this study was able to obtain more detailed results. Another difference is that the second regime of Badin and Domeisen's result is mono-fractal; however, the corresponding regime in the result of this study is a weak multi-fractal. This is because in this study, a stricter threshold was defined, as the ESS-MF-DFA can obtain a result with lower uncertainty.

3.1.3 Contrasting multi-fractal behaviors in tropospheric and stratospheric NAM variability

It has been shown that NAM variability is multi-fractal, in both the troposphere and the stratosphere (Figs. 2, 3). A natural question is whether there are different multi-fractal behaviors in the stratospheric and tropospheric NAM variability?

The most important feature in Figs. 2 and 3 is that the multi-fractal strengths over three scaling regimes are similar and nearly unchanged at a level from 1000 to 200 hPa. However, when the pressure level comes to 100 hPa or even

lower pressure levels, the stronger multi-fractal strength can be found in the middle range, especially in 10 hPa, where the strongest multi-fractal strength ($\Delta A = 2.28$) is reached. This unique multi-fractal behavior indicates that there are contrasting multi-fractal behaviors in NAM variability within the middle range between the troposphere and the stratosphere.

3.2 Origins of multi-fractal behavior in NAM variability

The causes of the marked multi-fractal behavior in NAM variability need to be investigated. Previous studies have suggested that there are two kinds of possible origins of multi-fractal behaviors. The first is due to a broad probability density function (PDF) of the values in the time series, and the second is due to different long-range correlations for small and large fluctuations (Kantelhardt et al. 2002; Movahed et al. 2006). To understand this multi-fractal behavior in NAM variability, it needs to be investigated whether the impacts of the probability distribution of NAM variability and the ordinal pattern in NAM variability play a role in the multi-fractal behaviors of NAM variability. Three surrogate methods were employed to find the answer to this question.

Since there are differences in the large and small fluctuations in the NAM variability over the all pressure levels

(Fig. 1), the PDF of NAM variability may vary greatly with the pressure level. A careful calculation shows that the PDF of NAM variability deviated from the normal distribution at all the pressure levels (Fig. 4a). The departures were found not only for small fluctuations in the NAM variability, but also for large fluctuations. Further calculations on higher order moments, such as skewness (defined as $skewness = \frac{E(x-\mu)^3}{\sigma^3}$, with the mean μ and standard deviation σ) and kurtosis (defined as $kurtosis = \frac{E(x-\mu)^4}{\sigma^4}$), confirmed that the NAM variability was not Gaussian distributed over nearly all the pressure levels (Fig. 4b, c). Whether these features dominated non-Gaussian distributions of the NAM variability contribute to the marked multi-fractal behavior in NAM variability requires further investigation.

The first surrogate method chosen in this study was a remapping procedure, where the ordinal pattern of the NAM index remained unchanged. For this procedure, the value of each point was replaced using random data with a standard Gaussian distribution. After this procedure, the surrogate data had the same autocorrelations as the NAM index, but the probability distribution of the surrogate was a standard Gaussian distribution (Movahed et al. 2006). The results from the remapped surrogate are shown in Fig. 5. If the multi-fractal behaviors were mostly due to the PDF contribution, then the ΔA of the remapped surrogates would significantly decrease (Movahed et al. 2006), with the multi-fractal strength near that of the mono-fractal feature. A comparison of the results given in Fig. 3 with those in Fig. 5 indicates that the broad PDF of NAM variability was not a key factor that would induce the marked multi-fractal behaviors in NAM variability. In particular, the multi-fractal behaviors in NAM variability were nearly unchanged over the troposphere (see Figs. 3a–d, 5a–d). The non-Gaussian PDF of NAM variability only played a minor role in the multi-fractal behaviors in NAM variability over

the stratosphere (see Figs. 3e–h, 5e–h). The maximum ΔA in 10 hPa was 1.55, which was reduced only 0.73, implying that the PDF did work, but it was not the primary reason for this observed multi-fractal feature.

The above-mentioned conclusions can be further confirmed by shuffling the surrogate results (see Fig. 6). The shuffling procedure keeps the PDF of the NAM variability unchanged but randomizes the order of the NAM variability by destroying the ordinal structure in the NAM variability. These structures include autocorrelations, both linear (two-point autocorrelation) and nonlinear. After shuffling, the distinctive multi-fractal behaviors near the scale of 345 were eliminated, and the ΔA was approximately 0.027 (smaller than $\Delta_{0.95} \approx 0.05$), which can be considered mono-fractal behavior. In addition, the multi-fractal behaviors due to PDF at both the small scale and the large scale were also removed except for the multi-fractal behaviors at left end of the small scale. This was due to some restrictions in the method based on DFA (Kantelhardt et al. 2001) and the partially non-Gaussian nature of NAM variability (figure not shown here).

A combination of the results of remapping and the shuffling surrogate showed that the origins of the marked multi-fractal behaviors in NAM variability were primarily due to linear and nonlinear autocorrelations in the NAM variability. Kantelhardt et al. (2002) mentioned that multi-fractal behaviors are related to the phase in the records of the Fourier transform. The phase randomized surrogate procedure (PRS) can randomize the phase, but keep the power spectral density (PSD) unchanged and remove most of the nonlinear behaviors, including the ones related to the non-Gaussian PDF and the nonlinear autocorrelation induced by phase correlation hidden in the data (Yuan et al. 2013). Figure 7 shows results from the PRS surrogates, from which it can be seen that the multi-fractal strength in the tropospheric NAM variability is nearly unchanged, but the multi-fractal strength

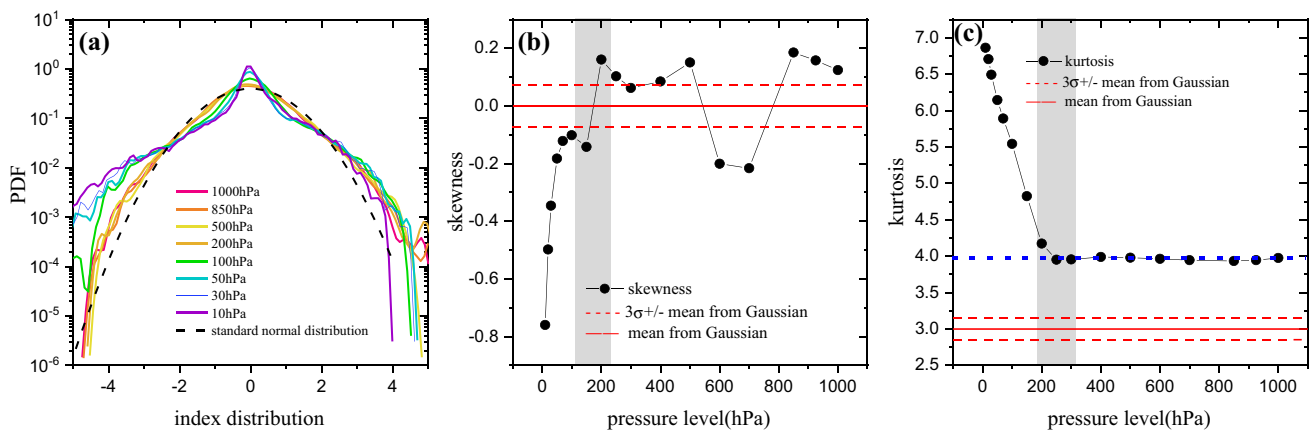


Fig. 4 a Probability distribution functions (PDF) of NAM index series at typical pressure levels and the moments: b skewness, and c kurtosis. The solid red lines in b and c represent the average of

skewness for 10,000 random series of Gaussian normal distributions, where three times the standard deviation is indicated by the red dash lines. The blue dash line denotes the stable regime in the troposphere

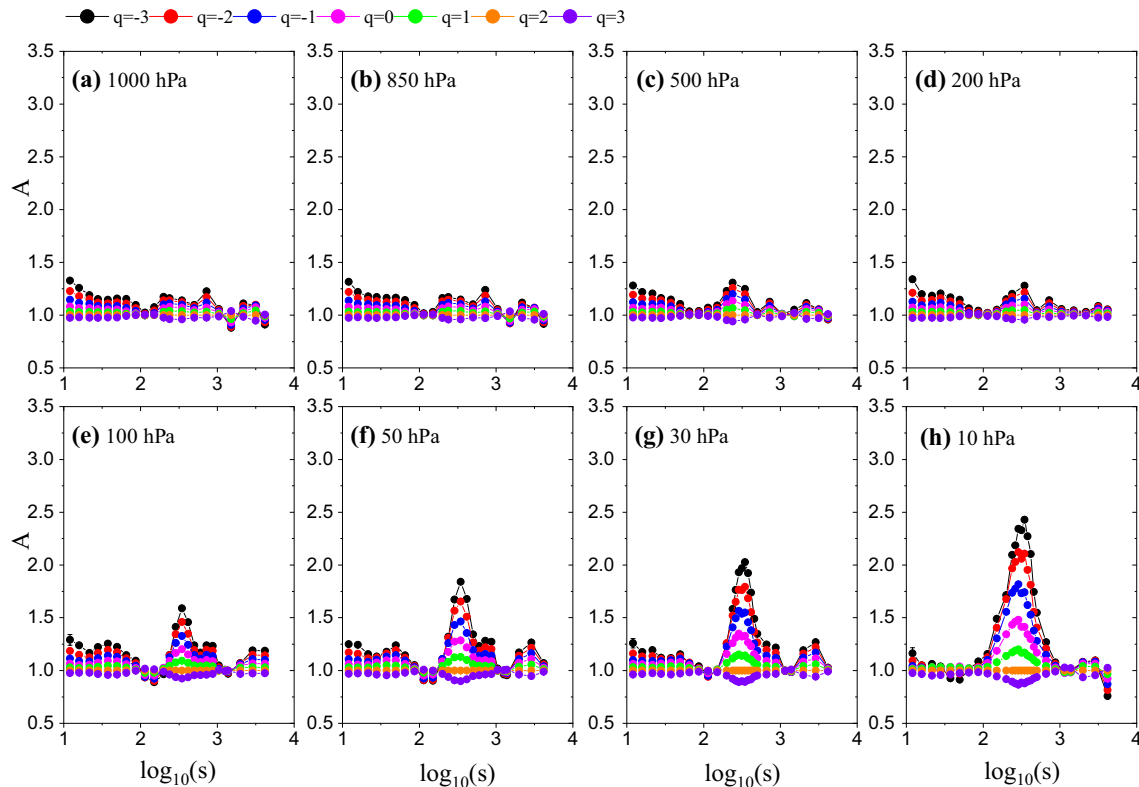


Fig. 5 Averaged local slope (A) from 100 remapping surrogates of the original NAM variability, with the standard deviation error bar (remapping process: keeping the original sequence of the NAM index, but replacing the data magnitude using random data with a

standard normal distribution) at various pressure levels: **a** 1000 hPa, **b** 850 hPa, **c** 500 hPa, **d** 200 hPa, **e** 100 hPa, **f** 50 hPa, **g** 30 hPa, **h** 10 hPa

in the stratospheric NAM variability is greatly reduced. The maximum ΔA is 0.35, found at 10 hPa. The magnitude of ΔA is reduced by 1.93, which is more than twice that from the remapping surrogate. The nonlinear autocorrelation induced by phase correlation of the data showed a significant multifractal feature.

A comparison of the results from the three types of surrogate methods showed that the multi-fractal behaviors were primarily caused by the ordinal structure of the NAM variability, which contained linear and nonlinear autocorrelations. In addition, the PDF of the NAM variability only played a minor role.

3.3 The mechanism of contrasting multi-fractal behaviors in tropospheric and stratospheric NAM variability

Results in the above sections showed that there were different multi-fractal behaviors in the stratospheric and tropospheric NAM variabilities. In addition, it was found that multi-fractal behaviors in the tropospheric NAM variability were primarily due to different linear autocorrelations in the large and small NAM variabilities. In contrast, the

multi-fractal behaviors in the stratospheric NAM variability were primarily due to nonlinear autocorrelations in the NAM variability, especially for the upper stratosphere. The question of why there were so many distinct differences in the multi-fractal behaviors in tropospheric and stratospheric NAM variability will be addressed from two aspects in the following subsections.

3.3.1 Contrasting basic statistics

A reinvestigation of the PDF of the NAM variability (Fig. 4a) shows that the NAM variability naturally fell into two clusters. One was nearly Gaussian, especially for small NAM variability (in the troposphere), the other was non-Gaussian for both large and small NAM variability (in the stratosphere). This marked difference is further clearly revealed in the higher moments, such as skewness (Fig. 4b) and kurtosis (Fig. 4c). The deviation from the Gaussian PDF for the tropospheric NAM variability is weaker compared to the stratospheric NAM variability. In particular, there is a clear dividing band (near 200 hPa) in the kurtosis (Fig. 4c), where the kurtosis for the tropospheric NAM variability saturates to a plateau of 4.0. In contrast, the kurtosis for the

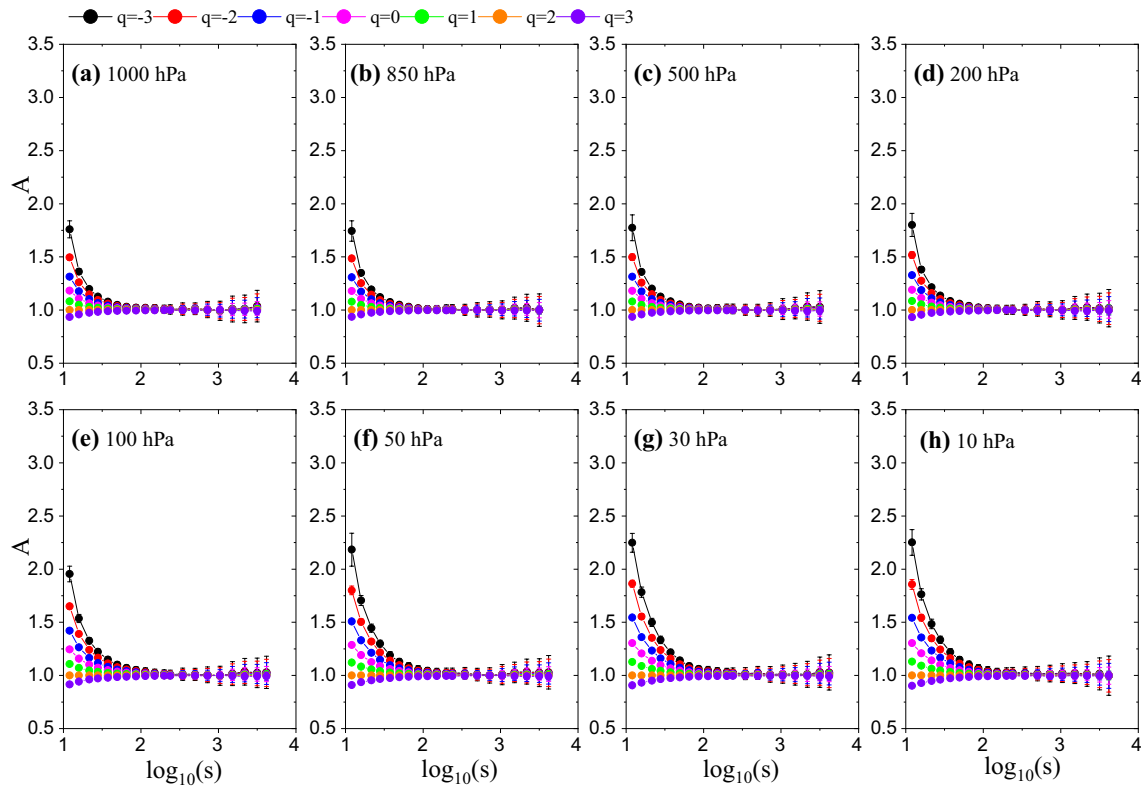


Fig. 6 Same as Fig. 5, but from the random shuffling surrogates (RS)

tropospheric NAM variability increases from 100 to 10 hPa. This distinguished higher correlation will certainly cause contrasting multi-fractal behaviors in the tropospheric and stratospheric NAM variability. This is why the multi-fractal behaviors in the tropospheric NAM variability were primarily due to the different linear autocorrelations in the large and small NAM variability, whereas the multi-fractal behaviors in the stratospheric NAM variability were primarily due to nonlinear autocorrelations in the NAM variability. The non-Gaussian PDF of the NAM variability contributed partially to the multi-fractal behaviors in the stratospheric NAM variability, but its contribution to the multi-fractal behaviors in the tropospheric NAM variability can be neglected (see Figs. 3, 5).

This contrasting stratospheric–tropospheric multi-fractal behavior is expressed directly in the variance (second moment) of the NAM variability. The variance from different frequency components in the NAM variability contributes to the total variance differently over different pressure levels. In particular, there is an apparent variance contribution ratio difference between the stratosphere and troposphere (Fig. 8). The variance contributions from the low-frequency band with a period of more than ten days shows an increase in the stratosphere. The lower the cutoff frequency, the more obvious this L-shape trend. When the

cutoff frequency is 90 or more days, the variance contributions have two regimes, with a constant value through the depth of the troposphere and strong variations through the stratosphere (Fig. 8b). Compared with the variance contributions from the low-frequency band, the variance contributions from the high-frequency band with a period of less than three days also has two regimes, with a stable state in the entire troposphere and varying considerably in the entire stratosphere (Fig. 8a). Both the variance contributions from the low-frequency band and the variance contributions from the high-frequency band show that the tropopause (near 200 hPa) is the transition band (consistent with what was derived in the PDF and kurtosis). In addition, there are different features below (troposphere) and above (stratosphere) this transition band. The large variance contribution comes from the high-frequency band over the troposphere, and this case corresponds to the relatively low multi-fractal features (weak nonlinearity). However, the large variance contribution from the low-frequency band over the stratosphere corresponds to the obvious multi-fractal features, which are an indicator of strong nonlinearity. This result is consistent with previous findings that enhanced predictability (more low-frequency oscillations) by increasing the nonlinearity in the ENSO and low-dimensional chaotic systems (Ye and

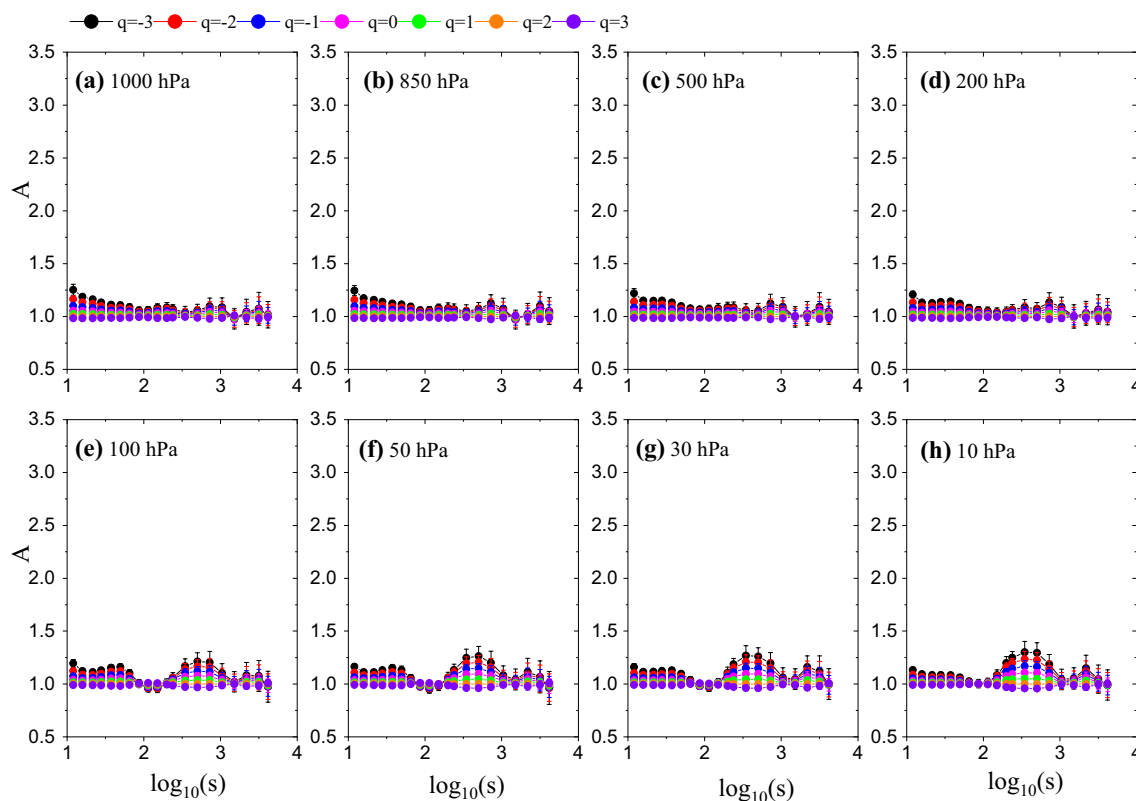
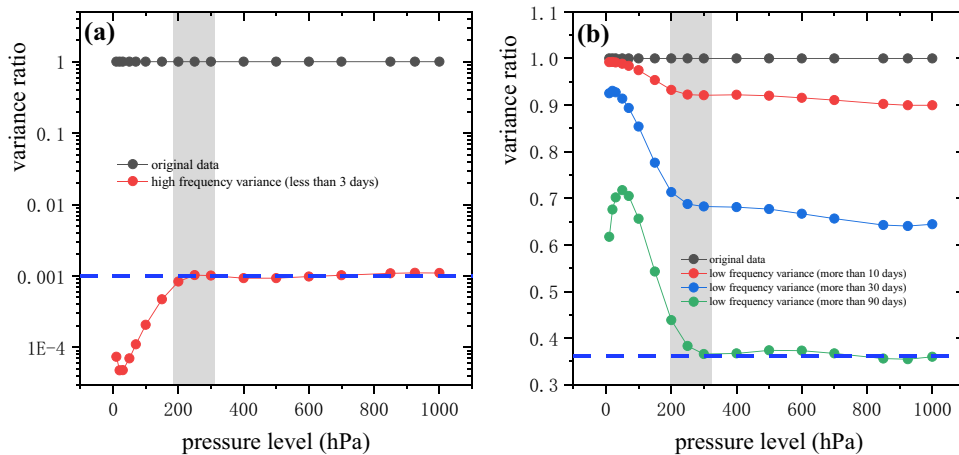


Fig. 7 Same as Fig. 5, but from the phase random surrogates (PRS)

Fig. 8 The variance ratio of different frequency components to the total components in the NAM index series at different pressure levels: **a** high frequency and **b** low frequency, with the original variance ratio being one. The blue dash line denotes the stable regime in the troposphere



Hsieh 2008). Therefore, it can also be inferred that the strong nonlinearity of the NAM variability corresponds to the dominant contribution of low-frequency activities and that the dominant low-frequency activities primarily occur in the stratosphere. In addition, low-frequency activities are always related to predictability (Ye and Hsieh 2008). This may be the primary reason why the contrasting multifractal behavior in the tropospheric and stratospheric NAM changes.

3.3.2 Contrasting cold/warm half-year differences

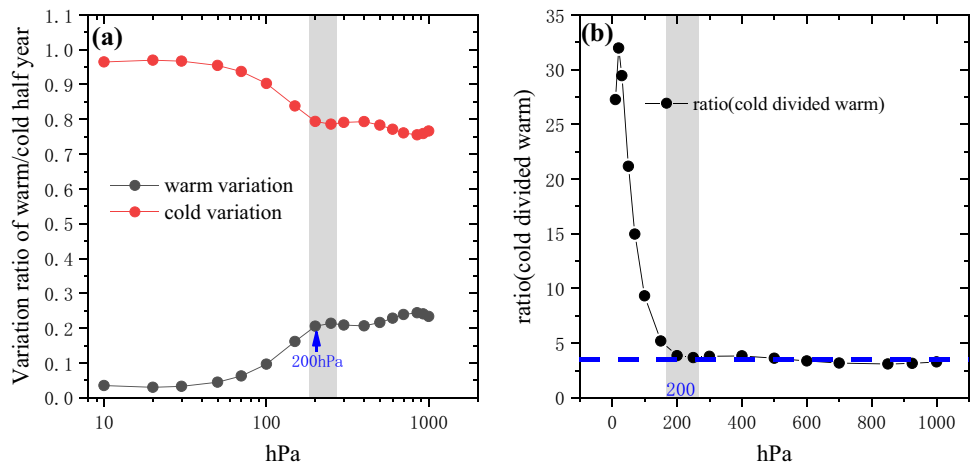
The second aspect that needed to be considered is the intra-annual and inter-annual NAM variability. In a review of the time series of the NAM index, the marked difference is not just between winter and summer, but the cold half year and the warm half year (Fig. 1). In this study, the cold half year contains six months consisting of November, December, January, February, March, and April, while the other six

months in the year are defined as the warm half year. The cold half-year variance contributed more than 76% to the total variance over all the pressure levels and more than 95% in the upper stratosphere (Fig. 9a), which is consistent with previous findings (Thompson and Wallace 1998; Baldwin 2001). The change from 200 to 10 hPa was significant, and the relative variance of the cold half year increased from 79.4 to 96.5%. The marked contribution differences in the warm and cold half years can be quantified using the variance ratio over the cold half-year to the warm half-year, and the cold half-year variance is nearly 33 times more than the warm half-year in upper stratosphere near 20 hPa (Fig. 9b). In addition, the two regimes (Fig. 9b) in the variance ratio emerge again with 200 hPa as the transition band, where the variance ratio is nearly constant over the troposphere, but varies greatly over the stratosphere. Additionally, in the dominated intra-annual NAM variability between the troposphere and the stratosphere, there are also clear inter-annual variations in the variance ratio. Importantly, the inter-annual variations in the variance ratio are much higher in the stratosphere than in the troposphere (Fig. 1). The contrasting intra-annual and inter-annual NAM variability are a possible cause that can induce the contrasting multi-fractal behaviors in the tropospheric and stratospheric NAM variability. In particular, the intermittent occurrence of large fluctuations during the cold half-year over the stratosphere can induce the stronger multi-fractal behaviors in the stratospheric NAM variability. However, the relative homogenous large and small fluctuations in the tropospheric NAM variability cannot lead to the stronger nonlinear autocorrelations in the marked multi-fractal behaviors.

The contrasting intra-annual NAM variability can be revealed in the linear features, such as the power spectrum distribution (PSD) and the autocorrelation function (ACF). The PSD of every cold/warm half-year during 1960–2017

was calculated and then the results were averaged for all of these 58 years, as shown in Fig. 10a, b. Similarly, the their ACFs are shown in Fig. 10d, e. The averaged PSD of the cold and warm half-years at 1000 hPa declines exponentially over a wide range (Fig. 10a, b). Similar results were found at other tropospheric levels (Fig. 10a, b). In addition, the PSD from different tropospheric levels nearly collapses into a single line (Fig. 10a, b). However, there are different PSD features over the low-frequency and high-frequency bands over the stratosphere. And most importantly, the exponentially decay is not within a single scaling range, but there are multiple (at least two) scaling ranges. These results indicate that the spectral features of the cold/warm half-year NAM variability over the troposphere and stratosphere are different. This difference can be shown more clearly in the PSD ratio of the cold to warm half-year plot (see Fig. 10c), where the results for the tropospheric NAM variability nearly collapse over nearly the entire range. However, there are many rich structures over different scales in the stratospheric NAM variability, more or less departed from those of the tropospheric NAM variability. There are distinguishable spectral features between the tropospheric and the stratospheric NAM variability, and the spectral structures are even more complicated in the stratospheric NAM variability. There are well corresponding relationships between the PSD and ACF, and the similar features can be found in the ACF figures (Fig. 10d–f). There are collapsed autocorrelation structures in the tropospheric NAM variability for both the cold and warm half-years, but there are scattered autocorrelation structures in the stratospheric NAM variability, especially for warm half-year (see Fig. 10e). The contrasting PSD and ACF in the tropospheric and the stratospheric NAM variability may have also contributed to the observed contrasting multi-fractal behaviors in the troposphere and the stratosphere.

Fig. 9 **a** The relative warm/cold half-year contribution of the NAM index to the year-round variance. **b** The variance ratio of the cold half-year to the warm half-year. The blue dash line denotes the stable regime in the troposphere



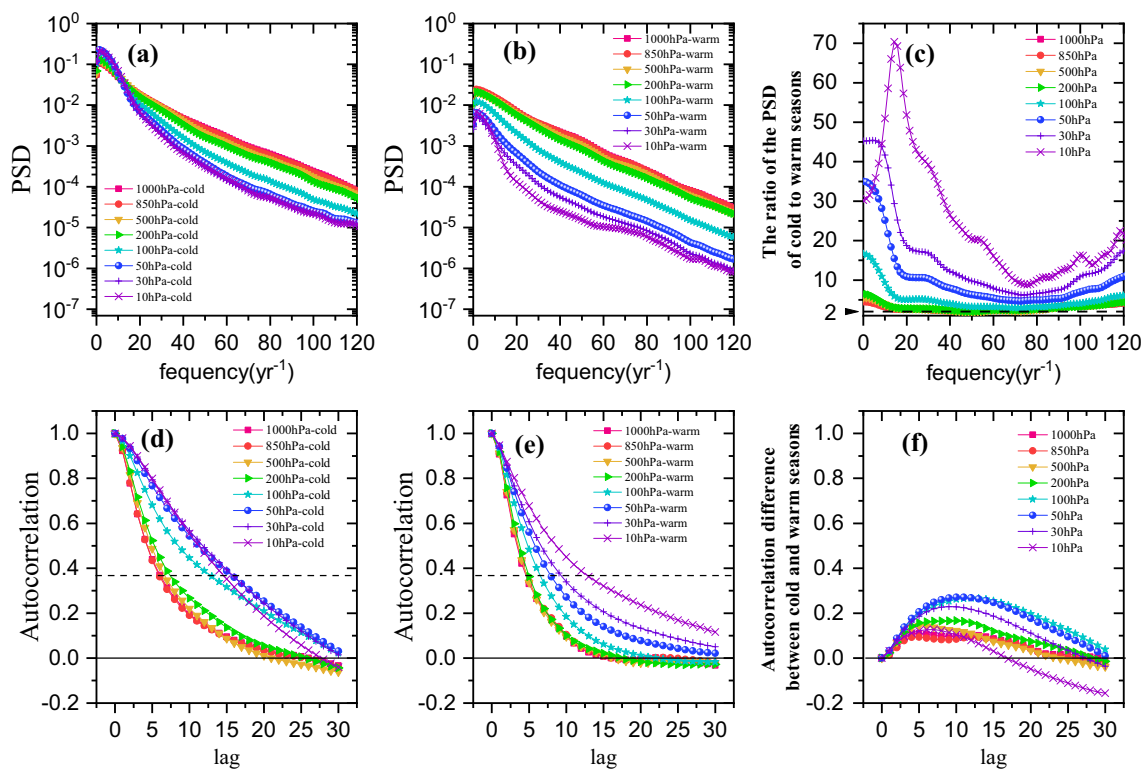


Fig. 10 The power spectrum distribution (PSD) and autocorrelation functions (ACF) of the warm/cold half-year NAM indices at typical various pressure levels: **a** averaged PSD for all the warm half years during 1960–2017 at typical pressure levels. **b** Same as **a** but for the cold half years. **c** The PSD ratio of the cold to the warm seasons with a minimum ratio of two. **d** The ACF difference between the cold and warm seasons

age autocorrelation functions over all the warm half years is in **d** the averaged ACF for all the warm half years during 1960–2017 at typical pressure levels. **e** Same as **d** but for the cold half years. **c** The PSD ratio of the cold to the warm seasons with a minimum ratio of two. **f** The ACF difference between the cold and warm seasons

4 Discussion and conclusion

In this study, the ESS-MF-DFA methods were used to detect the multi-fractal features in NAM indices. Although the MF-DFA method is widely used for the detection of multi-fractal features in time series, it *does not* work well for NAM variability. The results from the MF-DFA method are shown in Fig. 11, where there is no scaling range for each pressure level, especially for the tropospheric NAM variability. Since the power law assumption cannot be satisfied, the ESS-MF-DFA method may be a proper choice, where no power law assumption is made. Badin and Domeisen (2016) applied the MF-DFA method to different stratospheric variabilities. The fluctuation functions of a 10 hPa zonal wind using MF-DFA in their work were similar to those identified for the 10 hPa NAM index in Fig. 11h. Collectively, these results show that there are curved shapes in the fluctuation function over small scales and no clear scaling range. This may lead to a bias in the determination of the Hurst exponent, which may also cause a bias in the determination of the multi-fractal feature. However, the important conclusion put forth by Badin and Domeisen (2016) about a scaling transition of the scaling exponent for stratospheric variability in the Northern

Hemisphere is congruent with the results in this study of the transition band. Thus, it can be concluded that both methods give similar qualitative results; however, the ESS-MF-DFA method can provide more quantitative multi-fractal results.

The ESS-MF-DFA results for NAM variability showed that the NAM variability was multi-fractal in the troposphere and stratosphere. Three surrogate methods were employed to exploit the origin of the multi-fractal behaviors in NAM variability. The comparisons showed that the multi-fractal behaviors in the tropospheric NAM variability were primarily due to the different linear autocorrelations among large and small NAM fluctuations. In contrast, the multi-fractal behaviors in the stratospheric NAM variability were primarily due to nonlinear autocorrelations in the NAM indices, and both the non-Gaussian PDF of the NAM variability and the different linear autocorrelations among large and small NAM variabilities played a minor role.

Further studies revealed that there were very different multi-fractal behaviors in the tropospheric and stratospheric NAM variabilities. Different origins of the multi-fractal behaviors in the NAM variability in the tropospheric and stratospheric NAM indices explained why there are such contrasting multi-fractal behaviors for these parameters.

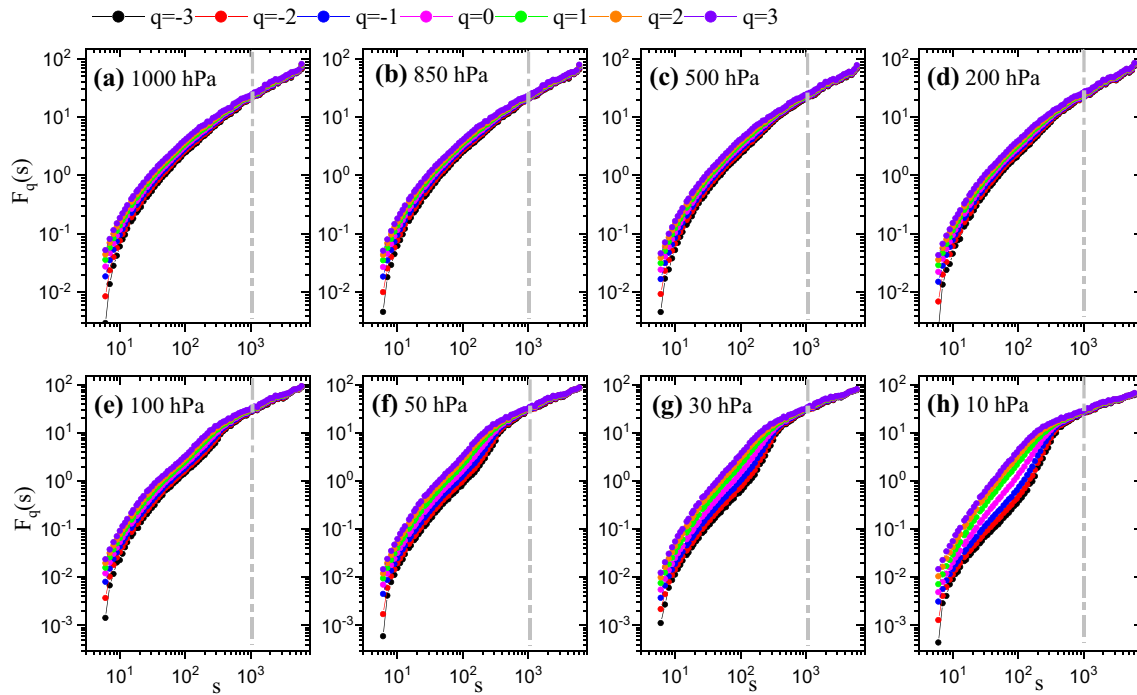


Fig. 11 Same as Fig. 2 but from the MF-DFA with q ($q = -3, -2, -1, 0, 1, 2, 3$). The grey dash line represents the same position in Fig. 2 with a scale of approximately $s = 10^3$

These contrasting multi-fractal behaviors were then examined from two aspects. Both the PDF of the NAM variability and the high-low frequency variance contribution ratio showed that there were two distinct regimes, one for the troposphere and the other for the stratosphere. Within the troposphere, both the PDF and related moments indicated that the tropospheric NAM variability was more homogeneous. Therefore, the multi-fractal strengths were weaker than those for the stratospheric NAM variability. The high-low frequency variance contribution ratio further confirmed these results. The other aspect that needed to be considered was the intra-annual and inter-annual NAM variability. There were contrasting cold and warm half-year NAM variations. The large fluctuations during the cold seasons imposed the most severe impacts on the low frequency variations in the upper stratosphere, which were associated with anomalies in the polar vortex. These anomalies were partially produced by the propagation of planetary waves that developed in the troposphere due to the zonal asymmetry of high-pressure levels (Feldstein and Franzke 2017). In addition, there were dominant inter-annual variations in the NAM variability with stratospheric sudden warming and strong polar vortex events. The contrasting intra-annual and inter-annual NAM variabilities are possible causes that induced the contrasting multi-fractal behaviors. In particular, intermittent occurrences of large fluctuations during the cold half-year over the stratosphere can induce stronger

multi-fractal behaviors in the stratospheric NAM variability. Therefore, it can be reasonably inferred that the marked seasonal difference in the tropospheric and stratospheric NAM variability causes contrasting multi-fractal behaviors. Badin and Domeisen (2014a) suggested that seasonality is not the reason for the multi-fractal structure of stratospheric variability. They compared the correlation and Lyapunov parameter from two simulations of stratospheric variability under different forcing conditions. One condition was a 360-day seasonal cycle, while the other condition was a perpetual winter condition. They found that the stratospheric variability in both simulations was multi-fractal. The results of this study are not in conflict with the results given by Badin and Domeisen (2014a), since the seasonality in their study was related to forcing, whereas the seasonality in this study was related to NAM variability.

Geopotential height data from the NCEP was used to calculate the NAM index. Some previous studies have shown that this dataset has significant problems near 10 hPa, which is near the pressures of the model lid (Gerber and Martineau 2018; Hitchcock 2019; Fujiwara et al. 2017). Although the NAM index obtained from the NCEP reanalyzed data set may be problematic at the top, the NAM index within the troposphere and lower-middle stratosphere is reliable, which is highly correlated (Pearson coefficient above 0.97) with a NAM index over each level from JRA-55 reanalysis. The main concern in this study was the contrasting multifractal

behaviors between the stratosphere and troposphere; however, this issue did not affect the main conclusions of this study. In fact, the calculation using the JRA-55 reanalysis was repeated, which had a much higher top and a more modern forecast model and assimilation system. Both reanalysis datasets had similar results (figures not shown), which indicated that the conclusion was robust. The quantitative difference between the NCEP and the JRA-55 reanalysis was that the strength of the multifractal features in the stratosphere was stronger using JRA-55 reanalysis. In addition, there were even stronger contrasting multifractal behaviors between the stratosphere and the troposphere using the JRA-55 reanalysis.

Previous studies have found that the behavior of stratospheric variability in the Northern Hemisphere is chaotic (Badin and Domeisen 2014a), and stratospheric variability exhibits different chaotic behaviors in the Northern and Southern Hemispheres (Badin and Domeisen 2014b). The findings in this study show that NAM variability is not only chaotic, but also multi-fractal. Furthermore, the chaotic behavior is not only spatial-dependent, but the multi-fractal strength is also height-dependent. PSD has been used as a popular method to infer chaotic behavior. Sigeti and Horsthemke (1987) stated that the falloff in the power spectra at high frequencies could be used to distinguish the time series of deterministic systems from those of stochastic systems. The PSD of a stochastic process has not been found to decay in the exponential form at the high frequency. Sigeti (1995) showed that the power spectra of deterministic chaotic systems will decay exponentially at high frequencies, and the exponential decay constant is roughly proportional to the sum of the positive Lyapunov exponents. The results of this study showed that all the PSDs of NAM in the cold/warm seasons decayed exponentially at high frequency (Fig. 10). Therefore, it can be inferred that chaos dominates the high frequency NAM variations over all levels. This result is consistent with the findings that deterministic chaotic behavior dominates the NAM variability at high frequencies due to the similar results that show that the power spectrums of the NAM index in wintertime and summertime at 1000 hPa decayed exponentially at a high frequency (Osprey and Ambaum 2011). Furthermore, it was shown in this study that mixed PSD structures in the stratospheric NAM variability were closely related to the stronger multi-fractal strength found in the stratospheric NAM variability. This result is also consistent with the dominated varying low-frequency variance contributions and the contrasting variance ratio of cold to warm half-years in the stratospheric NAM variability. Hence, from the PSD features, more can be learned than simply chaotic information. Since only the NAM index derived from EOFs was used to estimate the variability of the stratosphere and troposphere and is not a direct observable, the quantitative details of the index may

be different. Domeisen et al. (2018) addressed the problem of the different results that are obtained when one considers a direct observable or an index derived from EOFs. This also provides a direction for future research on comparisons between the NAM index and a direct observable from different viewpoints.

It is very important in the prediction of NAM changes that NAM propagates from the stratosphere to the troposphere, which is considered a precursor to abnormal tropospheric weather conditions. To better predict NAM variability, a comprehensive understanding of the behavior of NAM variability is required. Since high nonlinearity could be helpful in predictability (Ye and Hsieh 2008), it can be concluded that the strong multi-fractal features in NAM variability, as a nonlinear measure, is also an important indicator of predictability. Therefore, further work is required to assess the intrinsic predictability (the maximum degree of the predictability inherent to a given process) of the NAM variability over various levels. However, complicated multi-fractal behaviors, such as multiple scaling regimes over different scales, as well as marked contrasting warm–cold season features, may make the linear prediction strategy difficult to obtain high realizable predictability of NAM variations over the stratosphere. Huang and Fu (2019) found that multi-fractal patterns and nonlinearity in chaotic series can make impacts on the time series' prediction accuracy. Hence, the realizable predictability of NAM variations over the stratosphere should be reevaluated using practical prediction models or methods to see whether there are contrasting realizable predictability behaviors in tropospheric and stratospheric NAM variability. All these questions will be addressed in future studies.

Acknowledgements The authors thank the anonymous reviewers for their helpful suggestions for improving the readability of this paper. The authors acknowledge the supports from National Natural Science Foundation of China (nos. 41675049, 41475048).

References

- Ambaum MH, Hoskins BJ (2002) The NAO troposphere–stratosphere connection. *J Clim* 15(14):1969–1978. [https://doi.org/10.1175/1520-0442\(2002\)015%3c1969:TNTSC%3e2.0.CO;2](https://doi.org/10.1175/1520-0442(2002)015%3c1969:TNTSC%3e2.0.CO;2)
- Badin G, Domeisen DIV (2014a) A search for chaotic behavior in Northern Hemisphere stratospheric variability. *J Atmos Sci* 71(4):1494–1507. <https://doi.org/10.1175/JAS-D-13-0225.1>
- Badin G, Domeisen DIV (2014b) A search for chaotic behavior in stratospheric variability: comparison between the northern and southern hemispheres. *J Atmos Sci* 71(12):4611–4620. <https://doi.org/10.1175/JAS-D-14-0049.1>
- Badin G, Domeisen DIV (2016) Nonlinear stratospheric variability: multifractal de-trended fluctuation analysis and singularity spectra. *Proc R Soc A Math Phys* 472(2191):20150864. <https://doi.org/10.1098/rspa.2015.0864>

- Baldwin MP (2001) Annular modes in global daily surface pressure. *Geophys Res Lett* 28(21):4115–4118. <https://doi.org/10.1029/2001GL013564>
- Baldwin MP, Dunkerton TJ (1999) Propagation of the Arctic Oscillation from the stratosphere to the troposphere. *J Geophys Res* 104(D24):30937–30946. <https://doi.org/10.1029/1999JD900445>
- Baldwin MP, Dunkerton TJ (2001) Stratospheric harbingers of anomalous weather regimes. *Science* 294(5542):581–584. <https://doi.org/10.1126/science.1063315>
- Baldwin MP, Thompson DW (2009) A critical comparison of stratosphere–troposphere coupling indices. *Q J R Meteorol Soc* 135(644):1661–1672. <https://doi.org/10.1002/qj.479>
- Baldwin MP, Stephenson DB, Thompson DW, Dunkerton TJ, Charlton AJ, O'Neill A (2003) Stratospheric memory and skill of extended-range weather forecasts. *Science* 301(5633):636–640. <https://doi.org/10.1126/science.1087143>
- Bamzai AS (2003) Relationship between snow cover variability and Arctic Oscillation index on a hierarchy of time scales. *Int J Climatol* 23(2):131–142. <https://doi.org/10.1002/joc.854>
- Cai M, Ren RC (2007) Meridional and downward propagation of atmospheric circulation anomalies. Part I: Northern Hemisphere cold season variability. *J Atmos Sci* 64(6):1880–1901. <https://doi.org/10.1175/JAS3922.1>
- Cohen J, Foster J, Barlow M, Saito K, Jones J (2010) Winter 2009–2010: a case study of an extreme Arctic Oscillation event. *Geophys Res Lett* 37(17):L17707. <https://doi.org/10.1029/2010GL044256>
- Domeisen DIV, Badin G, Koszalka IM (2018) How predictable are the Arctic and North Atlantic oscillations? Exploring the variability and predictability of the Northern Hemisphere. *J Clim* 31(3):997–1014. <https://doi.org/10.1175/JCLI-D-17-0226.1>
- Feldstein B, Franzke CL (2017) Atmospheric teleconnection patterns. In: Franzke CL, O'Kane TJ (eds) *Nonlinear and stochastic climate dynamics*. Cambridge University Press, Cambridge, pp 54–104
- Fu ZT, Shi L, Xie FH, Piao L (2016) Nonlinear features of northern annular mode variability. *Physica A* 449:390–394
- Fujiwara M, Wright JS, Manney GL, Gray LJ, Anstey J, Birner T et al (2017) Introduction to the SPARC Reanalysis Intercomparison Project (S-RIP) and overview of the reanalysis systems. *Atmos Chem Phys* 17(2):1417–1452. <https://doi.org/10.5194/acp-17-1417-2017>
- Gerber EP, Martineau P (2018) Quantifying the variability of the annular modes: reanalysis uncertainty vs. sampling uncertainty. *Atmos Chem Phys* 18(23):17099–17117. <https://doi.org/10.5194/acp-18-17099-2018>
- Gerber EP, Baldwin MP, Akiyoshi H, Austin J, Bekki S, Braesicke P et al (2010) Stratosphere–troposphere coupling and annular mode variability in chemistry-climate models. *J Geophys Res*. <https://doi.org/10.1029/2009JD013770>
- Gillett NP, Graf HF, Osborn TJ (2003) Climate change and the North Atlantic oscillation. *Geophys Monogr Am Geophys Union* 134:193–210
- Gong DY, Wang SW, Zhu JH (2001) East Asian winter monsoon and Arctic oscillation. *Geophys Res Lett* 28(10):2073–2076. <https://doi.org/10.1029/2000GL012311>
- Gong DY, Kim SJ, Ho CH (2007) Arctic Oscillation and ice severity in the Bohai Sea, east Asia. *Int J Climatol* 27(10):1287–1302. <https://doi.org/10.1002/joc.1470>
- Hirata Y, Shimo Y, Tanaka HL, Aihara K (2011) Chaotic properties of the Arctic oscillation index. *SOLA* 7:33–36. <https://doi.org/10.2151/sola.2011-009>
- Hitchcock P (2019) On the value of reanalyses prior to 1979 for dynamical studies of stratosphere–troposphere coupling. *Atmos Chem Phys* 19(5):2749–2764. <https://doi.org/10.5194/acp-19-2749-2019>
- Hoerling MP, Hurrell JW, Xu T (2001) Tropical origins for recent North Atlantic climate change. *Science* 292(5514):90–92. <https://doi.org/10.1126/science.1058582>
- Huang Y, Fu Z (2019) Enhanced time series predictability with well-defined structures. *Theor Appl Climatol*. <https://doi.org/10.1007/s00704-019-02836-6>
- Kalnay E, Kanamitsu M, Kistler R, Collins W et al (1996) The NCEP/NCAR 40-year reanalysis project. *Bull Am Meteorol Soc* 77(3):437–472. [https://doi.org/10.1175/1520-0477\(1996\)077%3c0437:TNYRP%3e2.0.CO;2](https://doi.org/10.1175/1520-0477(1996)077%3c0437:TNYRP%3e2.0.CO;2)
- Kantelhardt JW, Koscielny-Bunde E, Rego HH, Havlin S, Bunde A (2001) Detecting long-range correlations with detrended fluctuation analysis. *Phys A* 295(3–4):441–454. [https://doi.org/10.1016/S0378-4371\(01\)00144-3](https://doi.org/10.1016/S0378-4371(01)00144-3)
- Kantelhardt JW, Zschiegner SA, Koscielny-Bunde E, Havlin S, Bunde A, Stanley HE (2002) Multifractal detrended fluctuation analysis of nonstationary time series. *Phys A* 316(1–4):87–114. [https://doi.org/10.1016/S0378-4371\(02\)01383-3](https://doi.org/10.1016/S0378-4371(02)01383-3)
- Keeley SPE, Sutton RT, Shaffrey LC (2009) Does the North Atlantic oscillation show unusual persistence on intraseasonal timescales? *Geophys Res Lett* 36(22):L22706. <https://doi.org/10.1029/2009GL040367>
- Kerr RA (1999) A new force in high-latitude climate. *Science* 284:241–242. <https://doi.org/10.1126/science.284.5412.241>
- Kerr RA (2001) Getting a handle on the North's El Niño. *Science* 294:494–495. <https://doi.org/10.1126/science.294.5542.494b>
- Kobayashi S, Ota Y, Harada Y, Ebata A, Moriya M, Onoda H et al (2015) The JRA-55 reanalysis: general specifications and basic characteristics. *J Meteorol Soc Jpn Ser II* 93(1):5–48. <https://doi.org/10.2151/jmsj.2015-001>
- Limpasuvan V, Hartmann DL (1999) Eddies and the annular modes of climate variability. *Geophys Res Lett* 26(20):3133–3136. <https://doi.org/10.1029/1999GL010478>
- Limpasuvan V, Hartmann DL (2000) Wave-maintained annular modes of climate variability. *J Clim* 13(24):4414–4429. [https://doi.org/10.1175/1520-0442\(2000\)013%3c4414:WMAMOC%3e2.0.CO;2](https://doi.org/10.1175/1520-0442(2000)013%3c4414:WMAMOC%3e2.0.CO;2)
- Movahed MS, Jafari GR, Ghasemi F, Rahvar S, Tabar MRR (2006) Multifractal detrended fluctuation analysis of sunspot time series. *J Stat Mech* 02:P02003. <https://doi.org/10.1088/1742-5468/2006/02/P02003>
- Nian D, Fu Z (2019) Extended self-similarity based multi-fractal detrended fluctuation analysis: a novel multi-fractal quantifying method. *Commun Nonlinear Sci Numer Simul* 67:568–576. <https://doi.org/10.1016/j.cnsns.2018.07.034>
- Osprey SM, Ambaum MH (2011) Evidence for the chaotic origin of Northern Annular Mode variability. *Geophys Res Lett* 38(15):L15702. <https://doi.org/10.1029/2011GL048181>
- Riddle EE, Butler AH, Furtado JC, Cohen JL et al (2013) CFSv2 ensemble prediction of the wintertime Arctic Oscillation. *Clim Dyn* 41:1099–1116. <https://doi.org/10.1007/s00382-013-1850-5>
- Sigeti DE (1995) Exponential decay of power spectra at high frequency and positive Lyapunov exponents. *Phys D* 82:136–153. [https://doi.org/10.1016/0167-2789\(94\)00225-F](https://doi.org/10.1016/0167-2789(94)00225-F)
- Sigeti D, Horsthemke W (1987) High-frequency power spectra for systems subject to noise. *Phys Rev A* 35(5):2276. <https://doi.org/10.1103/PhysRevA.35.2276>
- Simpson IR, Hitchcock P, Shepherd TG, Scinocca JF (2011) Stratospheric variability and tropospheric annular-mode timescales. *Geophys Res Lett*. <https://doi.org/10.1029/2011GL049304>
- Stockdale TN, Molteni F, Ferranti L (2015) Atmospheric initial conditions and the predictability of the Arctic Oscillation. *Geophys Res Lett* 42(4):1173–1179. <https://doi.org/10.1002/2014GL062681>
- Sun J, Ahn JB (2015) Dynamical seasonal predictability of the Arctic oscillation using a CGCM. *Int J Climatol* 35(7):1342–1353. <https://doi.org/10.1002/joc.4060>

- Thompson DW, Wallace JM (1998) The Arctic oscillation signature in the wintertime geopotential height and temperature fields. *Geophys Res Lett* 25(9):1297–1300. <https://doi.org/10.1029/98GL00950>
- Thompson DW, Wallace JM (2001) Regional climate impacts of the Northern Hemisphere annular mode. *Science* 293(5527):85–89. <https://doi.org/10.1126/science.1058958>
- Thompson DW, Baldwin MP, Wallace JM (2002) Stratospheric connection to Northern Hemisphere wintertime weather: implications for prediction. *J Clim* 15(12):1421–1428. [https://doi.org/10.1175/1520-0442\(2002\)015%3c1421:SCTNHW%3e2.0.CO;2](https://doi.org/10.1175/1520-0442(2002)015%3c1421:SCTNHW%3e2.0.CO;2)
- Wang J, Ikeda M (2000) Arctic oscillation and Arctic sea-ice oscillation. *Geophys Res Lett* 27(9):1287–1290. <https://doi.org/10.1029/1999GL002389>
- Wang L, Ting M, Kushner PJ (2017) A robust empirical seasonal prediction of winter NAO and surface climate. *Sci Rep* 7(1):279. <https://doi.org/10.1038/s41598-017-00353-y>
- Ye Z, Hsieh WW (2008) Enhancing predictability by increasing nonlinearity in ENSO and Lorenz systems. *Nonlinear Processes Geophys* 15:793–801. <https://doi.org/10.5194/npg-15-793-2008>
- Yuan N, Fu Z, Mao J (2013) Different multi-fractal behaviors of diurnal temperature range over the north and the south of China. *Theor Appl Climatol* 112:673–682. <https://doi.org/10.1007/s00704-012-0762-3>

Publisher's Note Springer Nature remains neutral with regard to jurisdictional claims in published maps and institutional affiliations.